



HAL
open science

Antimony isotopic fractionation during Sb(III) oxidation to Sb(V): Biotic and abiotic processes

Colin Ferrari, Eléonore Resongles, Marina Héry, Angélique Désoeuvre, Rémi Freydier, Sophie Delpoux, Odile Bruneel, Corinne Casiot

► To cite this version:

Colin Ferrari, Eléonore Resongles, Marina Héry, Angélique Désoeuvre, Rémi Freydier, et al.. Antimony isotopic fractionation during Sb(III) oxidation to Sb(V): Biotic and abiotic processes. *Chemical Geology*, 2023, 641, pp.121788. 10.1016/j.chemgeo.2023.121788 . hal-04267874

HAL Id: hal-04267874

<https://hal.science/hal-04267874>

Submitted on 2 Nov 2023

HAL is a multi-disciplinary open access archive for the deposit and dissemination of scientific research documents, whether they are published or not. The documents may come from teaching and research institutions in France or abroad, or from public or private research centers.

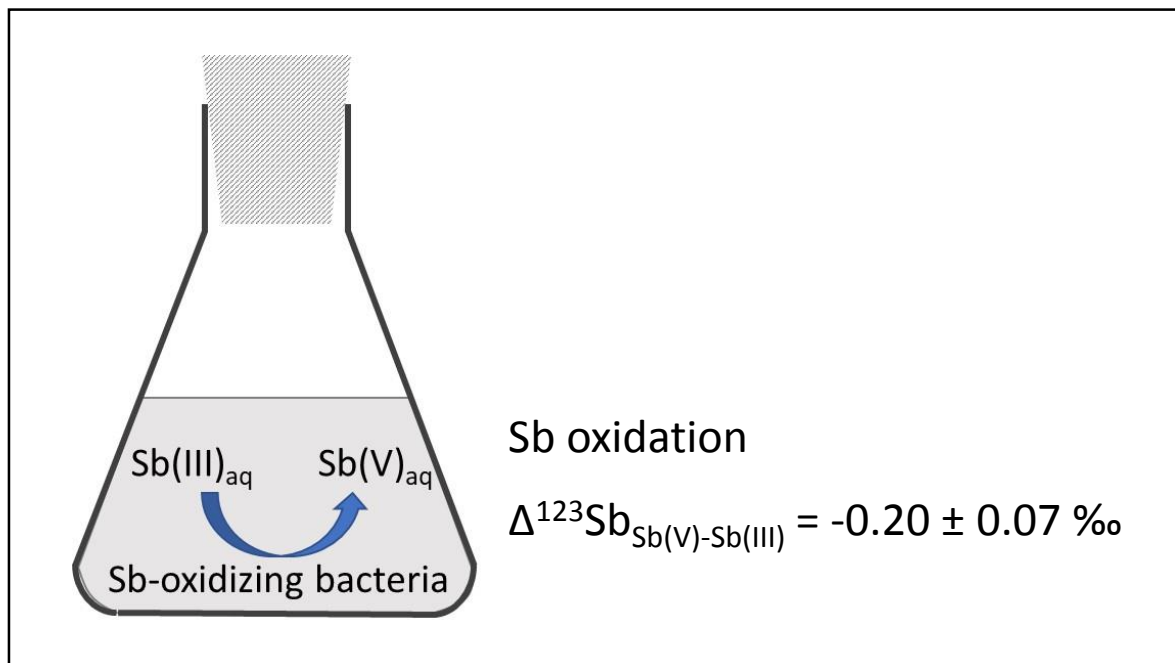
L'archive ouverte pluridisciplinaire **HAL**, est destinée au dépôt et à la diffusion de documents scientifiques de niveau recherche, publiés ou non, émanant des établissements d'enseignement et de recherche français ou étrangers, des laboratoires publics ou privés.

Chemical Geology

Antimony isotopic fractionation during Sb(III) oxidation to Sb(V): biotic and abiotic processes --Manuscript Draft--

Manuscript Number:	CHEMGE16198R1
Article Type:	Research paper
Keywords:	Antimony, isotopes, oxidation, bacteria, fractionation
Corresponding Author:	Corinne Casiot HydroSciences Montpellier FRANCE
First Author:	Colin Ferrari
Order of Authors:	Colin Ferrari Eléonore Resongles Marina Héry Angélique Desoeuvre Rémi Freydier Sophie Delpoux Odile Bruneel Corinne Casiot
Abstract:	<p>Oxidation of antimonite (Sb(III)) to antimonate (Sb(V)) plays an important role in the control of Sb mobility in aquatic systems. Fractionation of Sb isotopes ($^{123}\text{Sb}/^{121}\text{Sb}$) during Sb(III) oxidation has been investigated in the present study at concentrations relevant to mining environments. The isotopic composition ($\delta^{123}\text{Sb}$) of dissolved Sb(III) and Sb(V) species was analysed during biotic oxidation of Sb(III) at pH 6 and ~0.1 mM Sb. Biotic experiments used a <i>aioA</i> gene carrier bacterial strain of the genus <i>Ensifer</i> isolated from Sb-rich river sediments. Chemical oxidation experiments with H_2O_2 were also conducted either in NaNO_3 or HCl medium. During biotic oxidation, the Sb(V) produced was enriched in the light isotope compared to Sb(III), with an apparent fractionation factor $\Delta^{123}\text{Sb}_{\text{Sb(V)}-\text{Sb(III)}}$ of $-0.20 \pm 0.07 \text{ ‰}$. The $\Delta^{123}\text{Sb}$ value was independent of the oxidation kinetics within the range 0.03 to $0.05 \mu\text{mol.L}^{-1}\cdot\text{min}^{-1}$; the fractionation observed was rather attributed to kinetic effect that weakens over time in the experiments, although this hypothesis would require further investigation. During abiotic experiments in NaNO_3 medium, the Sb(V) produced was not isotopically fractionated relatively to Sb(III), while in HCl medium, the Sb(V) produced was enriched with the heavier isotope relatively to Sb(III), with a Rayleigh fractionation factor $\epsilon^{123}\text{Sb}$ of $+0.30 \pm 0.05 \text{ ‰}$. These differences were attributed to different reaction pathways involving multi-step reactions and either hydroxy- or chloride-Sb species. Altogether, these results showed a low fractionation of Sb isotopes during Sb(III) oxidation, although significant variability occurred according to experimental conditions. Further experimental research and confrontation with natural systems is necessary before applying Sb isotopes as process tracer in water.</p>

Graphical abstract



Antimony isotopic fractionation during Sb(III) oxidation to Sb(V): biotic and abiotic processes

Colin Ferrari^a, Eléonore Resongles^a, Marina Héry^a, Angélique Désoeuvre^a, Rémi Freydier^a, Sophie Delpoux^a, Odile Bruneel^a, Corinne Casiot^{a*}

^aHydroSciences Montpellier, Univ. Montpellier, CNRS, IRD, Montpellier, France

*Corresponding author

Mailing address : HydroSciences Montpellier UMR 5151

Faculté des Sciences Pharmaceutiques et Biologiques

Université de Montpellier, Bât. Hydropolis

15, avenue Charles Flahault

34093 Montpellier cedex 05, France

Email : corinne.casiot-marouani@umontpellier.fr

ORCID : 0000-0003-3318-5876

Abstract

Oxidation of antimonite (Sb(III)) to antimonate (Sb(V)) plays an important role in the control of Sb mobility in aquatic systems. Fractionation of Sb isotopes ($^{123}\text{Sb}/^{121}\text{Sb}$) during Sb(III) oxidation has been investigated in the present study at concentrations relevant to mining environments. The isotopic composition ($\delta^{123}\text{Sb}$) of dissolved Sb(III) and Sb(V) species was analysed during biotic oxidation of Sb(III) at pH 6 and ~ 0.1 mM Sb. Biotic experiments used a *aiOA* gene carrier bacterial strain of the genus *Ensifer* isolated from Sb-rich river sediments. Chemical oxidation experiments with H_2O_2 were also conducted either in NaNO_3 or HCl medium. During biotic oxidation, the Sb(V) produced was enriched in the light isotope compared to Sb(III), with an apparent fractionation factor $\Delta^{123}\text{Sb}_{\text{Sb(V)}-\text{Sb(III)}}$ of -0.20 ± 0.07 ‰. The $\Delta^{123}\text{Sb}$ value was independent of the oxidation kinetics within the range 0.03 to 0.05 $\mu\text{mol}\cdot\text{L}^{-1}\cdot\text{min}^{-1}$; the fractionation observed was rather attributed to kinetic effect that weakens over time in the experiments, although this hypothesis would require further investigation. During abiotic experiments in NaNO_3 medium, the Sb(V) produced was not isotopically fractionated relatively to Sb(III), while in HCl medium, the Sb(V) produced was enriched with the heavier isotope relatively to Sb(III), with a Rayleigh fractionation factor $\epsilon^{123}\text{Sb}$ of $+0.30 \pm 0.05$ ‰. These differences were attributed to different reaction pathways involving multi-step reactions and either hydroxy- or chloride-Sb species. Altogether, these results showed a low fractionation of Sb isotopes during Sb(III) oxidation, although significant variability occurred according to experimental conditions. Further experimental research and confrontation with natural systems is necessary before applying Sb isotopes as process tracer in water.

Keywords

Antimony, isotopes, oxidation, bacteria, fractionation

1. Introduction

Antimony is a contaminant of emerging concern. Environmental anthropogenic contamination has been evidenced on a global scale (Krachler *et al.*, 2005; Hong *et al.*, 2012). At the Earth's surface,

40 anthropogenic fluxes of Sb largely exceed natural fluxes ; they represent 80 % of total Sb flux, with
41 mining being the main contributing sector (Sen and Peucker-Ehrenbrink, 2012). Consequently, in
42 mining-impacted streams, Sb concentration can reach extreme values of ~0.1 mM (Zhu *et al.*, 2009;
43 Goix *et al.*, 2011). Dispersion of antimony downstream from mines is partly controlled by redox
44 processes. Antimony is present mainly under the reduced form (trivalent form Sb(III)) in sulphide
45 minerals (Vink, 1996), the most common being stibnite (Sb_2S_3). It is released into water upon sulphide
46 mineral dissolution in the form of the uncharged Sb(III) hydroxide species ($\text{Sb}(\text{OH})_3$) and tends generally
47 to be easily oxidized into Sb(V) ($\text{Sb}(\text{OH})_6^-$), even in relatively low Eh conditions (Filella *et al.*, 2001, 2002;
48 Mitsunobu *et al.*, 2006). This oxidation process controls Sb mobility; indeed, Sb(III) is more efficiently
49 retained onto suspended particulate matter and sediments than Sb(V) and can precipitate with iron
50 and other various oxides and hydroxides at high Sb concentration (Roper *et al.*, 2012; Johnston *et al.*,
51 2020). Sb(V) can combine with iron and oxygen to form tripuhyite, an efficient Sb sink in mine waters
52 (Leverett *et al.*, 2012), but it is mobile in the absence of iron (Resongles *et al.*, 2013). The abiotic
53 oxidation of Sb(III) by dissolved O_2 or H_2O_2 at environmentally relevant concentrations and acid or
54 neutral pH is very slow (e.g., the half-life of Sb(III) with 10^{-6} M H_2O_2 at pH 7 is ~ 3.2 years, Quentel *et al.*,
55 2004; Leuz *et al.*, 2006; He *et al.*, 2019). Some bacteria living in Sb-rich soils, sediments or acid mine
56 drainage can mediate this process (Li *et al.*, 2013, 2015, 2018; Nguyen and Lee, 2015; Terry *et al.*, 2015;
57 Nguyen *et al.*, 2017). Biotic Sb(III) oxidation occurs as a detoxification or respiration (providing energy
58 for growth) mechanism (Filella *et al.*, 2007; Lehr *et al.*, 2007; Li *et al.*, 2013, 2015; Wang *et al.*, 2015;
59 He *et al.*, 2019). Several oxidation paths involving Aio, Ano or ArsV oxidase (Wang *et al.*, 2015, Li *et al.*,
60 2015; He *et al.*, 2019; Zhang *et al.*, 2022) or extracellular superoxide (Wang *et al.*, 2022) have been
61 identified.

62 Change of redox state is generally a source of high isotopic fractionation for transition metals and
63 metalloids (Criss, 1999; Schauble, 2004; Wiederhold, 2015). The effect of oxidation on the isotopic
64 fractionation was experimentally studied for numerous metals and metalloids (Cr, Cu, Se, Te, Hg, Tl,
65 U...), although oxidation has been less studied than reduction (Johnson *et al.*, 2022), and there are no
66 experimental studies on Sb. Theoretical studies predicted equilibrium isotope fractionation between
67 oxidation states of Cr, Cu, Zn, Se, Hg, Tl, and Sb with an enrichment of heavy isotopes in the oxidized
68 species (Li and Liu, 2011; Ducher *et al.*, 2016; Liu *et al.*, 2021; Ferrari *et al.*, 2022). Field studies also
69 evidenced significant isotope fractionation associated to the oxidation of metals. Copper minerals that
70 have undergone numerous oxidation/reduction cycles show very large isotopic variations ($^{65}\text{Cu}/^{63}\text{Cu}$),
71 in the order of about 20 ‰ (Maréchal *et al.*, 1999; Larson *et al.*, 2003; Mathur *et al.*, 2005, 2009, 2010;
72 Asael *et al.*, 2007). Upon oxidative dissolution of Cr(III)-rich minerals to $\text{Cr}(\text{VI})_{\text{aq}}$, Gilleaudeau *et al.*
73 (2016) noted an enrichment of the aqueous phase in heavy isotopes by up to +1.77 ‰ ($^{53}\text{Cr}/^{52}\text{Cr}$). This
74 observation had also been made by Ellis *et al.* (2008) who quantified an isotopic fractionation of +1 ‰
75 upon oxidation of $\text{Cr}(\text{III})_s$ to $\text{Cr}(\text{VI})_{\text{aq}}$. This process did not follow a Rayleigh or kinetic fractionation but
76 rather an equilibrium fractionation, also observed by Wang *et al.* (2010). Johnson (2004) showed that
77 the reduction of Se(VI) into Se(IV) and Se(IV) into Se(0) is the main process fractionating selenium
78 isotopes. Fractionation ($^{80}\text{Se}/^{76}\text{Se}$) ranged from -7 to -12 ‰ (-3 to -5 ‰ for the biotic reaction) for the
79 reduction of Se(VI) to Se(IV) and from -6 to -12 ‰ (-6 to -9 ‰ for the biotic reaction) for the reduction
80 of Se(IV) to Se(0). In contrast, the reduction of Se(0) to Se(-II) and the oxidation (abiotic) of Se(IV) into
81 Se(VI) generated little or no apparent fractionation (Fry *et al.*, 1988; Johnson, 2004).

82 Biological processes can modify or even reverse the fractionation observed for abiotic redox
83 changes, forming lighter oxidized phases. For example, this is the case for copper, for which upon

84 oxidation of Cu sulphide in the presence of oxidizing bacteria, a fractionation factor $\Delta^{65}\text{Cu}_{\text{ox-red}}$ ranging
85 from -1‰ to -4.4‰ was observed, whereas for abiotic oxidation, a fractionation of +1 to +4‰ was
86 measured (Moynier *et al.*, 2017). This corroborates previous observations by Kimball *et al.* (2009),
87 demonstrating that the bacterial activity of *Acidithiobacillus ferrooxidans* oxidizing copper sulphide
88 ($\text{CuS} + 2\text{O}_2 \rightarrow \text{CuSO}_4$, (Torma and Habashi, 1972)) favours light ^{63}Cu isotope ($\Delta^{65}\text{Cu}_{\text{ox-red}} = -0.57 \pm 0.14$
89 ‰).

90 Few studies have investigated isotopic fractionation during antimony redox changes. Rouxel *et al.*
91 (2003) first showed that the reduction of Sb(V)_{aq} into $\text{Sb(III)}_{\text{aq}}$ induced a preferential enrichment of the
92 reduced phase with light ^{121}Sb isotope of around -0.9‰. Tanimizu *et al.* (2011) showed that dissolved
93 Sb(V) present in acid mine drainage (AMD) was around +0.35‰ heavier than the Sb(III) present in the
94 stibnite minerals in mine wastes from which the AMD originated. However, it was not clear which of
95 oxidation of Sb(III) into Sb(V) , dissolution of stibnite or adsorption most contributed to fractionation.
96 Mackinney, (2016) also observed an important isotopic fractionation during the reduction of Sb(V) into
97 Sb(III) and subsequent formation of $\text{Sb(III)}_2\text{S}_3$, with $\Delta^{123}\text{Sb}_{\text{Sb(V)-Sb(III)}}$ around +1.45‰; however, here again
98 it was not clear which of precipitation or reduction most contributed to the apparent fractionation. To
99 date, no work studied the isotopic fractionation of antimony during the oxidation of dissolved Sb(III)
100 into Sb(V) in controlled laboratory experiments.

101 The goal of this work was to quantify the direction and amplitude of Sb fractionation during biotic
102 and abiotic oxidation of $\text{Sb(III)}_{\text{aq}}$ into Sb(V)_{aq} in laboratory experiments. The Sb concentrations chosen
103 for experiments (~0.1 mM) were relevant to mining environments, and a bacterial strain originating
104 from a river sediment contaminated by a stibnite mine was used. These experiments represent a
105 crucial step in the development of Sb isotopes as geochemical tracer tool in mining environments and
106 in natural systems in general.

107 2. Material and methods

108 2.1 Reagents and materials

109 Sample preparation for analysis by ICP-MS, HG-ICP-MS and HG-MC-ICP-MS was carried out in a
110 class 10 000 cleanroom facility. Ultrapure water (Milli-Q®, resistivity > 18.2 MΩ cm, Q-POP Element
111 system, Millipore) was used for all experiments and reagent preparation. All consumables destined to
112 analysis and Sb isotope separation (e.g. sample bottles, tubes, SPE cartridge, pipette tips...) were
113 soaked in 10 % v/v analytical grade HCl or HNO_3 for 48 h and rinsed three times with ultrapure water
114 before use. Suprapur® ≥ 30 % w/w HCl (Merck®), and Analpure 65–69 % w/w HNO_3 (Analytika®) were
115 used for sample preparation and analysis. Other reagents and materials used in sample preparation
116 for ICP-MS, HG-ICP-MS, HPLC-ICP-MS and HG-MC-ICP-MS analysis are presented in the following
117 sections or described in detail in Ferrari *et al.* (2021).

118 2.2 Oxidation experiments

119 2.2.1 Biotic experiments

120 For biotic oxidation experiments, a bacterial strain called “RDB” isolated from a river sediment,
121 “Ravin des Bernès”, draining an ancient Sb mine (Felgerette mine, Collet-de-Dèze, France), and
122 containing 6942 mg.kg⁻¹ of Sb was used. The ability of this strain to oxidize Sb(III) into Sb(V) had been
123 shown in preliminary experiments, although the nature of the process involved (energy production or

124 detoxification) was not clear from our culture trials on minimum media using tartrate antimony.
125 Phylogenetic analysis indicated that strain RDB was affiliated to the *Ensifer/Sinorhizobium* group
126 (*Figure S1*). It possesses the *aioA* gene encoding the large sub-unit of an arsenite oxidase which can
127 also oxidize Sb(III). RDB was cultivated in CAsO1 medium at pH 6, supplemented with Sb(III). The sterile
128 CAsO1 medium was prepared as described in Battaglia-Brunet *et al.* (2002), with minor modifications:
129 the final concentration of $(\text{NH}_4)_2\text{SO}_4$ was $50 \text{ mg}\cdot\text{L}^{-1}$ and that of the yeast extract was $0.4 \text{ g}\cdot\text{L}^{-1}$. Sb(III) was
130 added from a 0.1 M Sb(III) solution made with potassium antimony(III) oxide tartrate trihydrate
131 (Extrapure, Merck®). The filtered sterile Sb(III) solution was added to the cooled medium after
132 autoclaving to a final concentration of 0.5 mM (for pre-cultures) or 0.1 mM (for biotic oxidation
133 experiments); the exact Sb(III) concentration in the cultures at t_0 was determined by HPLC-ICP-MS.
134 Three biotic oxidation experiments, called RDB0, RDB1-3 and RDB4 were conducted, including one
135 (RDB1-3) in triplicate and with two types of abiotic controls (Abio1-3 and Control-1-3) in parallel. For
136 each experiment, the bacterial suspension used as inoculum was collected from a pre-culture in
137 exponential growth phase, centrifuged and resuspended in Sb(III)-free medium. Considering the fast
138 kinetics (all Sb(III) oxidized within less than 80 h), and the complex logistics of sampling, separation and
139 analysis, the inoculum size and the starting time of experiments were optimized to obtain samples
140 covering a wide range of percentage of oxidized Sb(III). After addition of the inoculum (1 ml), the initial
141 optical density at 600 nm was almost similar in the three experiments, ranging from 0.020 to 0.032.
142 Experiment RDB4 was inoculated half day after experiment RDB1-3, in order to compensate for the
143 lack of sampling during the night. Two kinds of abiotic controls were made. Abio1-3 corresponded to
144 the culture medium inoculated with autoclaved bacterial pellet; it was conducted in triplicate.
145 Control1-3 corresponded to the culture medium without inoculum, in triplicate. All cultures (300 ml)
146 were performed in acid-decontaminated, autoclaved Erlenmeyer flasks and protected with a cellulose
147 cap. They were incubated at 28 °C with shaking at 100 rpm. Samples (1 mL) were collected at different
148 times (every hour, when possible, during the first day) for OD (600 nm) measurement (*Figure S2*),
149 analysis of redox Sb speciation (Sb(III) and Sb(V) concentrations) and isotopic composition
150 determination of aqueous Sb(III) and Sb(V). Samples for speciation and isotope analyses were filtrated
151 ($<0.22 \mu\text{m}$) and frozen until analysis as a previous test confirmed that no Sb oxidation or precipitation
152 occurred using this mode of conservation.

153 2.2.2 Chemical oxidation

154 Chemical oxidation was performed using hydrogen peroxide (Suprapur 30 % w/w H_2O_2 , Merck®)
155 as oxidant. This strong oxidizing agent was chosen because abiotic oxidation by oxygen is too slow,
156 indeed, no significant Sb(III) oxidation by O_2 was observed within 200 days in the pH range 4-10
157 (Quentel *et al.*, 2004; Leuz and Johnson, 2005). A first experiment was conducted with $\sim 0.1 \text{ mM}$ Sb(III)
158 at pH 6, as in the biotic experiment. The methodology of Quentel *et al.*, 2004 and Leuz *et al.* (2006)
159 was applied, except that the ionic strength was fixed with 0.01 M NaNO_3 rather than NaCl to avoid
160 complexation of Sb with chloride. We could not use CAsO1 medium in abiotic experiments (for a strict
161 comparison with biotic experiments) because the selective Sb(III) separation protocol used for biotic
162 samples (see section 2.3) was not applicable in the presence of H_2O_2 due to a fast Sb(III) oxidation
163 during the sample conditioning step. Alternatively, we took advantage of the selectivity of hydride
164 generation toward the Sb(III) species to directly measure the isotope ratio $^{123}\text{Sb}/^{121}\text{Sb}$ of Sb(III) without
165 separation step. This direct measurement was not compatible with the introduction of complex culture
166 medium matrix. Our preliminary experiments showed that in a solution containing a mixture of Sb(III)
167 and Sb(V) at a concentration of $2 \mu\text{g}\cdot\text{L}^{-1}$ in 0.01 M NaNO_3 , 100 % of Sb(III) was converted into volatile

168 hydride, while a maximum of 10 % of Sb(V) was converted. This result was consistent with previous
169 studies (Xi *et al.*, 2015). The first chemical oxidation experiment was carried out in duplicate and
170 conducted as follows. 20 ml of 0.15 M H₂O₂ solution were added to 30 ml of 0.14 mM Sb(III) in 0.01 M
171 NaNO₃ solution at pH 6 (adjusted using a 0.1 M NaOH solution) to reach final concentrations of 0.08
172 mM Sb(III) and 60 mM H₂O₂. Vials were immediately agitated and maintained at constant temperature
173 (21 °C), with no direct sunlight. An aliquot was collected every 26 min, immediately diluted in 3 M HCl
174 to reach a 2 µg.L⁻¹ concentration of Sb, and analysed immediately by HG-MC-ICP-MS. This
175 measurement provided Sb(III) isotopic composition, together with Sb(III) concentration, using semi-
176 quantitative analysis, by comparison with the signal intensity of the isotopic standard solution
177 prepared at 2 µg.L⁻¹ of Sb (from the mono-elemental solution at 1000 µg mL⁻¹ of Sb in 20 % w/w HCl,
178 batch number 24-175SBX, SPEX CertiPrep). The solution drained from the gas-liquid separator
179 (hydride-generation module) was sequentially collected for determination of the isotopic composition
180 of Sb(V), after reduction into Sb(III) in 0.5 % w/v potassium iodide and ascorbic acid, as described
181 before (Ferrari *et al.*, 2021).

182 A second chemical oxidation experiment was carried out using on-line HG-MC-ICP-MS analysis. For
183 this, a solution containing 10⁻⁴ mM Sb(III) in 3 M HCl was used. Hydrogen peroxide was added at a
184 concentration of 0.05 mM at different time-intervals before analysis. The solution drained from the
185 gas-liquid separator was sequentially collected and analysed for Sb(V) isotopic composition
186 determination, as described previously.

187 2.3. Separation of Sb(III) and Sb(V) in biotic experiments

188 To analyse the isotope composition of Sb(III) and Sb(V) in the complex bacterial culture medium,
189 physical separation of these two species is needed. For this, Sb(III) was selectively separated from Sb(V)
190 on 0.2 g of thiol-functionalized mesoporous silica powder (hereafter referred to as TSP) at pH ~10, in
191 1 mL polypropylene SPE cartridges fitted with polyethylene frits (Supelco®). A modified elution
192 protocol from Ferrari *et al.* (2021) was used (Table 1). Selective sorption conditions were based on
193 sorption properties of Sb(III) and Sb(V) species on thiol-functionalized cotton fibers defined by Yu *et*
194 *al.* (1983); Sb(V) is not sorbed at basic pH while Sb(III) is fully sorbed in this pH range. Samples
195 containing around 500 ng of antimony were passed through the TSP column after pH adjustment to
196 ~10 (using a 5.7 mM NH₄OH solution, Suprapur, Merck®). The selectivity of the procedure has been
197 tested with pure Sb(V) or Sb(III) solutions; the results can be seen in Table S1. The selective recovery
198 yields for Sb(V) and Sb(III) in elution steps 3 and 7 of the elution scheme were found between 92 and
199 104 %, respectively. In this modified protocol, the cleaning step 1 was carried out with ultrapure water
200 rather than 6 M HCl to avoid Sb(V) reduction. A blank sample showed that despite this modification,
201 the amount of Sb in elution step 7 was lower than 1 ng (<1% of total purified Sb). Antimony
202 concentration was determined in elution fractions 3+4 (corresponding to Sb(V)) and 7 (corresponding
203 to Sb(III)) by HG-ICP-MS. This allowed to calculate the proportion of Sb(III) and Sb(V) in the samples.
204 The value was compared with the result of HPLC-ICP-MS analysis. Differences of ~3.5 % on average,
205 was obtained between HPLC measurements and physical separations of Sb(III) and Sb(V) (Table S2).

206 *Table 1: Elution scheme for the separation of the Sb(III) and Sb(V) species using thiol-functionalized silica powder modified*
207 *from Ferrari et al. (2021).*

Step	Volume (mL)	Eluent	Notes
1 Cleaning	10	Ultrapure water	

2	Conditioning	10	NH ₄ OH 5.7 mM	
3	Sample loading	10	NH ₄ OH 5.7 mM	Sb(V) collection (steps 3 and 4)
4	Rinsing	5	NH ₄ OH 5.7 mM	
5	Washing	5	0.5 M HCl	
6	Washing	6	2.5 M HCl	
7	Sb(III) elution	6	6 M HCl	Sb(III) collection

208

209

2.4 Analytical methods

210 All the analyses (HPLC-ICP-MS, HG-ICP-MS, HG-MC-ICP-MS) were performed on the AETE-ISO
 211 platform (OSU OREME, University of Montpellier) using iCAP Q ICP-MS and Neptune Plus MC-ICP-MS
 212 (Thermo Scientific®).

213 Monitoring of Sb(III) and Sb(V) concentrations in biotic experiments was carried out by High-
 214 Performance Liquid Chromatography coupled to ICP-MS (HPLC-ICP-MS) as described in Resongles *et*
 215 *al.* (2013).

216 HG-ICP-MS and HG-MC-ICP-MS instrument informations and measurement settings were taken
 217 from Ferrari *et al.* (2021), with slight modifications; for HG-MC-ICP-MS, short-term shifts in the Sb
 218 isotope ratio due to overpressure in the gas-liquid separator (Ferrari *et al.*, 2021) were attenuated by
 219 suppressing additional gas and adjusting sample gas for hydride generation. For better signal stability
 220 and reproducibility, the Sb concentration was adjusted at 2 µg L⁻¹ for all HG-MC-ICP-MS measurements.
 221 For the chemical oxidation experiments, the analysis time in HG-MC-ICP-MS was decreased in order to
 222 generate more measurement points during the oxidation kinetics, each measurement has been
 223 diminished from 80 cycles of 4.194 seconds (Ferrari *et al.*, 2021) to 40 cycles of 4.194 s (on samples
 224 and standards).

225

2.5 Nomenclature

226 Isotope composition is expressed as δ¹²³Sb (Equation 1) and corresponds to the average value for
 227 three independent isotopic measurements if not specified otherwise.

$$228 \quad \delta^{123}\text{Sb}(\text{‰}) = \left(\frac{\left(\frac{^{123}\text{Sb}}{^{121}\text{Sb}}\right)_{\text{sample}} - \left(\frac{^{123}\text{Sb}}{^{121}\text{Sb}}\right)_{\text{mean std}}}{\left(\frac{^{123}\text{Sb}}{^{121}\text{Sb}}\right)_{\text{mean std}}} \right) \times 1000 \text{ (Eq. 1)}$$

229 where $\left(\frac{^{123}\text{Sb}}{^{121}\text{Sb}}\right)_{\text{mean std}}$ is the average of Sb isotope ratio of the Sb isotope standard solution measured
 230 before and after the sample (Sb 1000 µg mL⁻¹ in 20 % w/w HCl, batch number 24-175SBX, SPEX).

231 The apparent fractionation factor Δ¹²³Sb_{Sb(V)-Sb(III)} between the isotopic composition of Sb(III) and Sb(V)
 232 can be calculated according to Equation 2.

$$233 \quad \Delta^{123}\text{Sb}_{\text{Sb(V)-Sb(III)}} = \delta^{123}\text{Sb}_{\text{Sb(V)}} - \delta^{123}\text{Sb}_{\text{Sb(III)}} \text{ (Eq. 2)}$$

234

235 Rayleigh fits of the isotopic composition $\delta^{123}\text{Sb}_{\text{Sb(III)}}$ and $\delta^{123}\text{Sb}_{\text{Sb(V)}}$ at different fractions (f) of remaining
 236 Sb(III) were utilized to determine the Rayleigh fractionation factor ($\epsilon^{123}\text{Sb}$) in permil, using Equation 3
 237 (Wiederhold, 2015):

$$238 \quad \delta^{123}\text{Sb}_{\text{Sb(III)}} \approx \delta^{123}\text{Sb}_{\text{Sb(III)0}} + \epsilon^{123}\text{Sb} \times \ln f \text{ (Eq.3)}$$

239 where $\delta^{123}\text{Sb}_{\text{Sb(III)0}}$ represents the $\delta^{123}\text{Sb}$ value of Sb(III) at the beginning of the experiment and f
 240 represents the fraction of remaining Sb(III).

241 The isotopic evolution of the cumulative Sb(V) product (Equation 4) is described by:

$$242 \quad \delta^{123}\text{Sb}_{\text{Sb(V)}} = \delta^{123}\text{Sb}_{\text{Sb(III)0}} + \epsilon^{123}\text{Sb} \times \ln f - (\epsilon^{123}\text{Sb} \times \ln f)/(1-f) \text{ (Eq.4)}$$

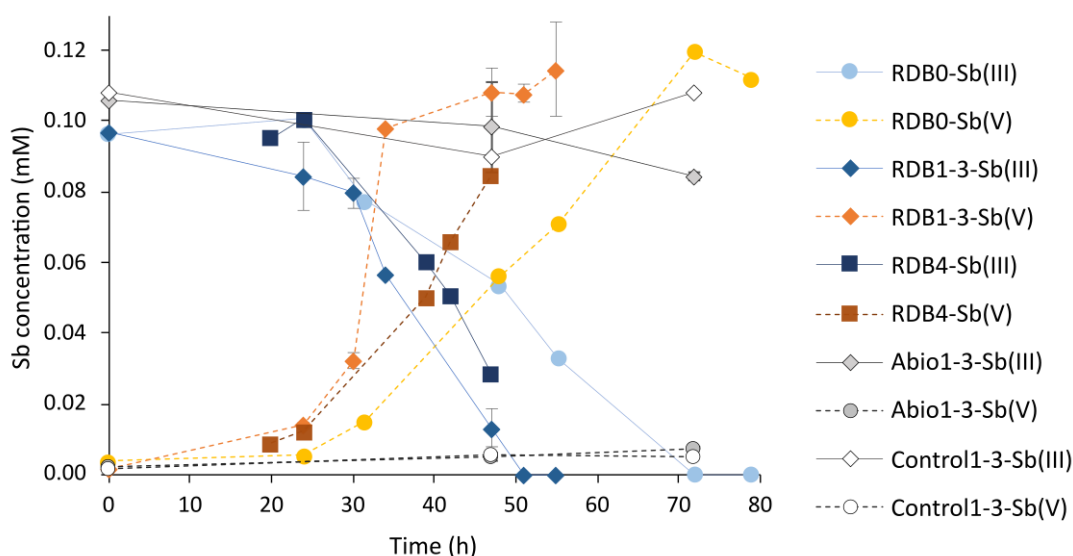
243

244 3. Results

245 3.1 Biotic oxidation

246 3.1.1 Evolution of Sb(III) oxidation

247 Biotic oxidation of Sb(III) in the three experiments started after a lag period of about 20 h (Figure
 248 1). It was decoupled from the exponential bacterial growth phase, which systematically occurred
 249 before 20 h, according to OD measurements (Figure S2). Sb(III) oxidation was completed within 51 h
 250 (in experiment RDB1-3) to 70 h (in experiment RDB0), which corresponded to oxidation rate values of
 251 $0.05 \mu\text{mol.L}^{-1}.\text{min}^{-1}$ (RDB1-3), $0.04 \mu\text{mol.L}^{-1}.\text{min}^{-1}$ (RDB4) and $0.03 \mu\text{mol.L}^{-1}.\text{min}^{-1}$ (RDB0) (Figure S3).
 252 Control and abiotic experiments showed less than 8 % of Sb(III) oxidized after 72 hours. This confirmed
 253 that Sb(III) oxidation was mediated by bacteria. The sum of Sb(III) and Sb(V) did not decrease during
 254 the experiments, showing that no precipitation of Sb occurred.



255

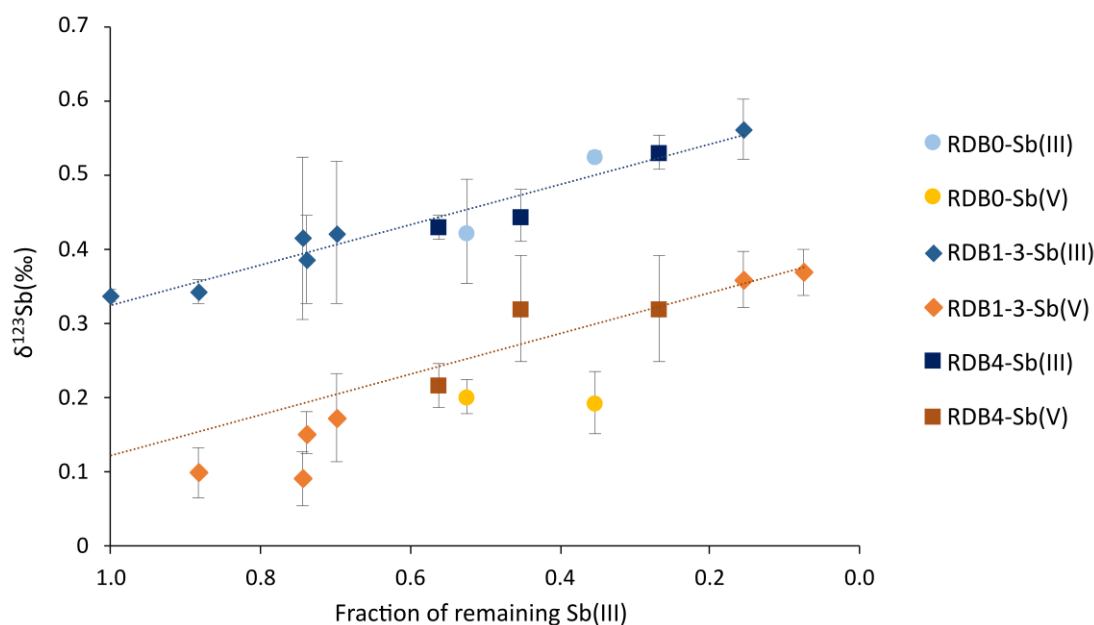
256 *Figure 1: Evolution of the concentration of Sb(III) (solid line) and Sb(V) (broken line) in biotic (coloured symbols) experiments*
 257 *RDB0, RDB1-3 and RDB4 and abiotic (grey and white symbols) experiments Abio1-3 and Control1-3. Data for RDB1-3, Abio1-*
 258 *3 and Control1-3 are represented by the mean values of triplicate experiments and associated standard error.*

259

3.1.2 Isotopic composition of Sb(III) and Sb(V)

260 The variation of $\delta^{123}\text{Sb}$ as a function of the fraction of remaining Sb(III) showed a significant
 261 fractionation of Sb isotopes between the Sb(III) species and its biotic oxidation product (Figure 2). The
 262 oxidation of Sb(III) seemed to follow a closed system equilibrium model (Figure 2), rather than a
 263 Rayleigh fractionation model (Figure S4); almost parallel increase of the isotopic composition of Sb(III)
 264 and Sb(V) occurred as the fraction of remaining Sb(III) decreased (Figure 2). The apparent fractionation
 265 factor $\Delta^{123}\text{Sb}_{\text{Sb(V)-Sb(III)}}$ was determined at -0.20 ± 0.07 ‰ on average, with a preferential enrichment in
 266 light isotope in the product Sb(V). The same trend was observed for the three experiments; there was
 267 no significant influence of the oxidation kinetics on the fractionation factor $\Delta^{123}\text{Sb}_{\text{Sb(V)-Sb(III)}}$, which was
 268 similar for RDB0 ($\Delta^{123}\text{Sb}_{\text{Sb(V)-Sb(III)}} = -0.28 \pm 0.08$ ‰), RDB1-3 ($\Delta^{123}\text{Sb}_{\text{Sb(V)-Sb(III)}} = -0.25 \pm 0.04$ ‰) and RDB4
 269 ($\Delta^{123}\text{Sb}_{\text{Sb(V)-Sb(III)}} = -0.18 \pm 0.05$ ‰). It is noteworthy that in the experiment RDB1-3, the apparent
 270 fractionation is slightly higher during the first stage of the reaction ($f > 0.6$, $\Delta^{123}\text{Sb}_{\text{Sb(V)-Sb(III)}} = -0.26 \pm 0.04$
 271 ‰) compared to the final stage of the reaction ($f < 0.2$, $\Delta^{123}\text{Sb}_{\text{Sb(V)-Sb(III)}} = -0.20 \pm 0.04$ ‰).

272



273

274

275 *Figure 2: Isotopic composition ($\delta^{123}\text{Sb}$) of Sb(III) (blue tones) and Sb(V) (yellow-orange) during biotic oxidation as a function*
 276 *of fraction of remaining Sb(III) in solution. The dashed parallel lines correspond to an equilibrium isotope fractionation with*
 277 *the average fractionation factor $\Delta^{123}\text{Sb}_{\text{Sb(V)-Sb(III)}}$ of -0.20 ± 0.07 ‰.*

278

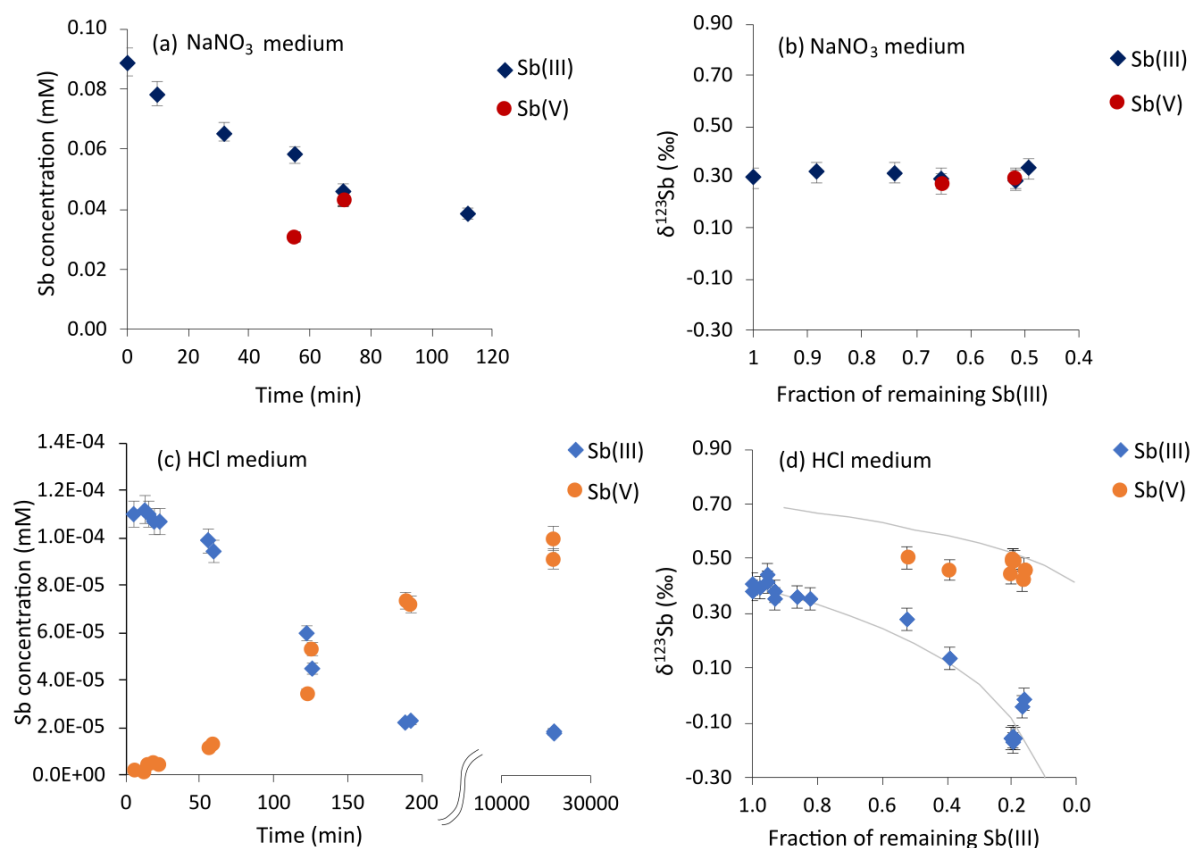
279

3.2 Chemical oxidation with H_2O_2

280 Chemical Sb(III) oxidation with ~ 0.1 mM Sb(III) in NaNO_3 medium reached 51 % after 112 minutes
 281 (Figure 3a), corresponding to $0.3 \mu\text{mol.L}^{-1}.\text{min}^{-1}$ (Figure S3). The initial isotopic composition of Sb(III)
 282 ($\delta^{123}\text{Sb} = 0.30 \pm 0.04$ ‰) was identical to that measured in the biotic experiments at t_0 ($\delta^{123}\text{Sb} = 0.33 \pm$
 283 0.04 ‰). The experiment did not show significant fractionation during the oxidation reaction progress
 284 between remaining Sb(III) ($\delta^{123}\text{Sb} = 0.33 \pm 0.04$ ‰) and produced Sb(V) ($\delta^{123}\text{Sb} = 0.29 \pm 0.02$ ‰) (Figure
 285 3b). Similar results were obtained in a preliminary chemical oxidation experiment in which a physical
 286 separation of Sb(III) and Sb(V) with TSP had been done prior to Sb isotope measurement (Table S3).

287 Chemical Sb(III) oxidation with 10^{-4} mM Sb(III) in 3 M HCl showed similar proportion of Sb(III)
 288 oxidized, with 39 % Sb(III) oxidized within 131 min (Figure 3c) and $0.0004 \mu\text{mol}\cdot\text{L}^{-1}\cdot\text{min}^{-1}$ (Figure S3).
 289 After 190 min, Sb(III) oxidation slowed down, and there was still 16 % of Sb(III) remaining after 15 days
 290 (Figure 3c). The isotopic composition of Sb(III) initially present in the HCl 3 M solution averaged $0.40 \pm$
 291 0.02‰ , Figure 3d). The Sb(V) accumulated in solution was enriched in the heavier isotope compared
 292 to remaining Sb(III) (Figure 3d). The evolution of $\delta^{123}\text{Sb}$ was better represented by a Rayleigh model,
 293 with ϵ value of 0.3‰ , although the cumulative Sb(V) data did not perfectly matched theoretical
 294 Rayleigh curve (Figure 3d).

295



296

297 *Figure 3: Evolution of the concentration of Sb(III) and Sb(V) (left) and isotopic composition $\delta^{123}\text{Sb}$ (right) in chemical oxidation*
 298 *experiments with ~ 0.1 mM Sb(III) in 0.01 M NaNO_3 and 60 mM H_2O_2 (a, b) and with 10^{-4} mM Sb(III) in 3 M HCl and 0.05 mM*
 299 *H_2O_2 (c, d). The grey lines in figure (d) represent the theoretical isotopic composition of reactant Sb(III) and cumulative product*
 300 *Sb(V) considering a Rayleigh fractionation model with ϵ value = 0.3‰ . Error bars correspond to the analytical uncertainty (\pm*
 301 *0.04‰) determined in Ferrari et al. (2021).*

302

303

4. Discussion

304

4.1 Isotopic fractionation related to biotic Sb(III) oxidation

305 The contribution of bacterial activity on the Sb(III) oxidation rate was clearly demonstrated by the
 306 significant differences obtained between the biotic experiments and the controls without living
 307 bacteria. Biotic oxidation induced a light isotope enrichment of the Sb(V) product compared to the
 308 Sb(III) reactant. For the three biotic experiments, the evolution of $\delta^{123}\text{Sb}$ for the remaining Sb(III) and

309 the produced Sb(V) was best fitted with an equilibrium fractionation model (Figure 2) rather than
310 Rayleigh model (Figure S4), and the slightly different kinetics between experiments RDB0, RDB1-3 and
311 RDB4 did not produce significantly different fractionation factors $\Delta^{123}\text{Sb}_{\text{Sb(V)}-\text{Sb(III)}}$ (Figure 2). This
312 suggests that the isotopic fractionation does not depend on the kinetics of biotic Sb(III) oxidation in
313 the conditions of this study. This might be related to the rather slow kinetics of the biotic oxidation
314 experiments compared to chemical oxidation experiments (one order of magnitude difference).
315 However, there is a body of evidence that lean against an equilibrium fractionation.

316 First of all, there are several points in Figure 2 that do not fit the equilibrium model within the
317 given measurement uncertainties. For example, the earliest three Sb(V) points are all significantly
318 below the best-fit model.

319 Considering the enzymatic-catalyzed character of the biotic oxidation process, an isotopic
320 fractionation of kinetic origin was expected. Indeed, biological processes are kinetically controlled
321 (since they involve bond-breaking in enzymatic reactions) and may thus induce significant kinetic
322 isotope effects. The bacterial strain used in our study possess the *aioA* gene involved in Sb(III)
323 oxidation. Therefore, the involvement of an enzyme in the oxidation reaction was expected to
324 influence the reaction pathway, and thus the isotope distribution between the reactant and the
325 product, which can lead to kinetic isotopic fractionation.

326 Bacterial-catalyzed reduction reactions for elements such as Cr and Se, whose behavior is close to
327 that of antimony showed significant kinetic isotope fractionation. Bacterial reduction of selenium
328 oxyanions generated kinetic isotope fractionation by 3-12 ‰ (Johnson, 2004; Schilling *et al.*, 2020). For
329 biological chromium oxyanions reduction, fractionation was 0.4-7.6 ‰ (Zhang *et al.*, 2018). Both
330 elements showed enrichment in the light isotope in the product during these experiments. An
331 important difference with the present study is that the processes involved during Se and Cr oxyanions
332 reduction goes through unidirectional phase changes from dissolved to solid, without back-reaction.
333 Such unidirectional processes were prone to imprint significant isotope fractionation, which
334 contrasted with the present study where reactants and products remained in the aqueous phase.
335 Furthermore, the biologically-catalyzed reaction pathway may have an important influence on the
336 isotope fractionation. Schilling *et al.* (2020) have shown that different strains or incubation conditions
337 produced different fractionation factors during biological selenium reduction, in relation with the
338 reduction pathway, and the amplitude of fractionation is controlled by the rate-limiting step. Several
339 oxidation pathways, related to different oxidases, have been identified among Sb-oxidizing bacteria.
340 The AioA protein is a periplasmic or intermembrane enzyme (in the inner membrane) (Mukhopadhyay
341 *et al.*, 2002; Santini and vanden Hoven, 2004); it has the capacity to oxidize Sb(III) aerobically, without
342 the need for Sb(III) to enter the cell cytoplasm. In the present study, the location of the AioA enzyme
343 in the periplasm may imply diffusion of Sb(III) in the inter-membrane space prior to oxidation. This may
344 be the rate-limiting step of the whole oxidation process. Considering that diffusion produces
345 smaller isotope fractionation than oxidation (Rodushkin *et al.*, 2004), the whole reaction path in our
346 biological oxidation experiments may generate small kinetic fractionation amplitude.

347 If equilibrium fractionation is considered in the present study, the direction of fractionation, with
348 isotopically light Sb(V) relative to the Sb(III), contradicts well-known theoretical considerations. The
349 higher valence species of many redox-sensitive elements have shorter, stiffer, higher energy bonds
350 than the lower valence species ; thus the heavier isotopes are enriched in the higher valence species if

351 equilibrium is achieved (Stephens *et al.*, 2021). Thermodynamic calculations by Ferrari *et al.* (2022)
352 showed this is true for Sb as well. Antimony(V)-oxides minerals are preferentially enriched in the heavy
353 ^{123}Sb isotope than Sb(III)-oxides ; the equilibrium fractionation factor $\Delta^{123}\text{Sb}_{\text{Sb(V)}-\text{Sb(III)}}$ is about +1.2 ‰
354 between senarmonite ($\text{Sb(III)}_2\text{O}_3$) and Sb(V) oxide $\text{Sb(V)}_2\text{O}_5$ (Ferrari *et al.*, 2022). In the present biotic
355 experiments, the redox and ionic structure change from a tetragonal pyramid in $\text{Sb(OH)}_{3,\text{aq}}$ to
356 octahedral configuration in $\text{Sb(OH)}_{6,\text{aq}}^-$ was expected to produce important Sb isotope fractionation,
357 and enrichment in the heavier isotope in Sb(V). A small fractionation in opposite direction suggests
358 another or a masking mechanism.

359 It is commonly observed that bacteria synthesize organic compounds that can complex metals
360 and metalloids. Sb(III) and Sb(V) species form stable complexes with a variety of small organic acids
361 (Filella and May, 2005; Tella and Pokrovski, 2009). One can suggest that complexation of Sb(III) and
362 Sb(V) with organic compounds released by bacteria fractionated Sb isotopes in the opposite direction
363 than oxidation. Preferentially light Zn, Cd, and Hg isotopes bind to thiol groups (Wiederhold, 2015 ;
364 Wigganhauser *et al.*, 2022) or carboxylic groups (for Cd, Ratié *et al.* (2021)) at equilibrium. However, it
365 seems quite unlikely that the expected equilibrium fractionation of more than 1 per mil between Sb(V)
366 and Sb(III), with Sb(V) enriched in heavier isotopes, could be completely reversed by complexation with
367 organic ligands. Furthermore, considering the greater tendency of Sb(III) to form Sb-S bonds, compared
368 to Sb(V), the fractionation between Sb(V) and Sb(III) complexed with organic thiol groups at
369 equilibrium would increase.

370 Alternatively, the observed pattern in the data could be the result of a kinetic isotope effect that
371 decreases in magnitude during the experiment. Variation of isotopic fractionation can be hypothesized
372 because the medium where bacteria evolve is subjected to changes such as variations in the physico-
373 chemical conditions and medium toxicity, evolution in the physiological state of the microbes as the
374 experiments proceed and the Sb(V) and Sb(III) concentrations change. Such a change in the isotopic
375 fractionation has been observed during microbial Se reduction experiments; as the Se species
376 concentrations changed, fractionation increased (Herbel *et al.*, 2000). This latter pattern was
377 attributed to enzymatic Se reduction steps becoming rate limiting upon non-respiratory pathways such
378 as Se transport across the cell membrane. Altogether, the present data suggest a kinetic effect
379 explaining variation of the isotopic composition over time. Further research is needed to validate this
380 hypothesis.

381

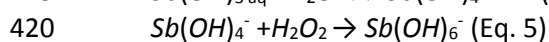
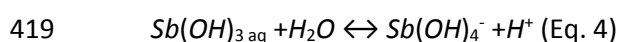
382 **4.2 Isotopic fractionation related to chemical Sb(III) oxidation with H_2O_2**

383 The Sb(III) chemical oxidation experiments showed little or no isotopic fractionation, with a
384 maximum enrichment of + 0.3 ‰ in heavy isotope in the Sb(V) product. The low fractionation reported
385 here differed from previous experimental studies dealing with Sb redox transformations. Rouxel *et al.*
386 (2003) reported a shift of $\Delta^{123}\text{Sb}_{\text{Sb(III)}-\text{Sb(V)}}$ around -0.55 to -0.9 ‰ during abiotic Sb(V) reduction by iodide
387 in HCl medium, in relation with a kinetic isotope effect. Mackinney (2016) showed a higher kinetic
388 isotope fractionation of -1.42 ‰ during Sb(V) reduction by sulfide. There was no experiment reporting
389 Sb isotope fractionation during oxidation reaction in the literature.

390 Comparison with other redox-sensitive elements such as selenium and chromium may help to
391 interpret the results since these elements share common geochemical properties with Sb. Johnson
392 (2004) showed no measurable Se isotope fractionation during oxidation of dissolved Se(IV) into Se(VI)
393 with H_2O_2 in strongly basic solution. Regarding chromium, Zink *et al.* (2010) showed small (+0.2 ‰)
394 isotopic fractionation during oxidation of dissolved Cr(III) to dissolved Cr(VI) in alkaline media, using

395 H₂O₂ as the oxidant; the reaction favoured heavy Cr isotopes in Cr(VI). These results were in line with
396 our Sb(III) chemical oxidation experiments with 10⁻⁴ mM Sb(III) in HCl medium that showed a slight
397 enrichment in the heavier isotope in the Sb(V) product ($\epsilon^{123}\text{Sb} = +0.3 \text{ ‰}$). Some $\delta^{123}\text{Sb}$ values for the
398 Sb(V) product diverged from the Rayleigh model, as observed by Zink *et al.* (2010) for Cr(III) oxidation.
399 Zink *et al.* (2010) interpreted the poor fitting of experimental data to Rayleigh-type function by the
400 involvement of unstable reactional intermediates Cr(IV) and Cr(V) and the divergence of the process
401 from a single, unidirectional reaction. Indeed, kinetic isotope fractionation depends on the mechanism
402 of reaction and the rate of individual steps. In our experiments, the Sb speciation and oxidation
403 mechanism can be proposed by comparison with the study of Quentel *et al.* (2004). These authors
404 investigated the oxidation of Sb(III) by H₂O₂ in a mildly acidic hydrochloric acid medium (0.5 M HCl).
405 Quentel *et al.*, (2004) suggested that the reaction of Sb(III) oxidation by H₂O₂ goes through the
406 formation of chlorine by H₂O₂, followed by the oxidation of Sb(III) by the chlorine formed. Chloro-
407 complexes of Sb(III) (SbCl₄⁻) and Sb(V) (SbCl₆⁻) are expected in 3 M HCl medium (Bonner and Goishi,
408 1961). Quentel *et al.* (2004) suggested possible formation of transition species containing chloride
409 bridges between SbCl₆⁻ and SbCl₄⁻ that would facilitate electron transfer at high HCl concentration. In
410 our abiotic experiments, the HCl concentration is even higher than in the Quentel *et al.* (2004)
411 experiments, thus such a mechanism might be involved. Therefore, a multiple-step reaction and
412 formation of intermediate species may control the magnitude and direction of Sb isotope fractionation
413 in our chemical Sb(III) oxidation experiment in HCl medium.

414 In the NaNO₃ medium, Sb isotope fractionation during Sb(III) oxidation was not significant. The
415 mechanism was probably completely different from that occurring in HCl medium. In NaNO₃ medium
416 at pH 6, Sb(III) is present as Sb(OH)_{3 aq}; the undissociated Sb(OH)_{3 aq} does not react with H₂O₂, the
417 formation of Sb(OH)₄⁻ is needed for the reaction to take place (Quentel *et al.*, 2004; Leuz *et al.*, 2005),
418 as follows:



421 The reaction rates of individual steps may influence Sb isotope fractionation, the extent of which
422 being controlled by the rate-limiting step. In NaNO₃ medium, Eq. 4 (hydrolysis) may be the rate limiting
423 step controlling Sb isotope fractionation, thus producing low fractionation compared to Eq. 5.

424 These results support observations made for other isotopic systems (Cr, Se). It is generally
425 expected that oxidation reaction produces a lower fractionation than reduction reaction (Johnson et
426 al, 2022). For reduction reactions, the valence decreases and thus the equilibrium and kinetic effects
427 of the individual steps both work in the same direction. This leads to an isotopically light product as a
428 rule. For oxidation reaction, the kinetic and equilibrium effects of individual reaction steps potentially
429 oppose each other, thus, we expect the oxidation reactions to have fractionations that are smaller in
430 magnitude than reduction reactions. Indeed, certain reaction steps inside the overall process could
431 produce isotopically heavy products (if they are close to equilibrium, with valence increasing) or could
432 produce light products (if the forward reaction dominates for that step), Thus, the overall process,
433 which is the combination of potentially positive and negative steps (positive epsilon values or negative
434 values) would produce a low fractionation.

435 Altogether, the present data suggest that small fractionations like those seen in the present study
436 could be the rule for Sb oxidation.

437

438 4.3 Environmental implications

439 Our observations have implications for the interpretation of antimony isotopic composition in
440 aquatic environments highly enriched with Sb. The fractionation produced during biological oxidation
441 is in the same direction than that produced by sorption of Sb(V) onto iron minerals (Zhou *et al.*, 2023),
442 which is another major process involved in Sb behaviour in contaminated waters. This must be
443 considered for interpretation of Sb isotopes dynamic in the environment. Furthermore, the
444 fractionation factors obtained in laboratory conditions with a pure bacterial strain must be confronted
445 to the apparent fractionation factors in real natural environments where more complex bacterial
446 populations are likely to interact with Sb. The Sb isotope fractionation may vary according to the
447 bacterial strain, in relation with different metabolic pathways, as seen for selenium reduction (Schilling
448 *et al.*, 2020).

449 Concerning abiotic oxidation, additional conditions should be investigated as various complex
450 multi-step reaction processes can generate different apparent isotopic fractionation for a same
451 reaction (Johnson *et al.*, 2022). In particular, considering the role of iron and manganese
452 (oxyhydr)oxides in both redox transformations and sorption of Sb in the environment (Belzile *et al.*,
453 2001; Resongles *et al.*, 2013; Guo *et al.*, 2018), Sb isotope fractionation related to oxidation by these
454 phases should be investigated. For example, Dwivedi *et al.* (2022) recently showed that oxidation of
455 aqueous Se(IV) by Mn oxide birnessite produces Se(VI) which is enriched in the lighter isotope relative
456 to Se(IV), attributed to a kinetic effect, with a fractionation factor of -2.33‰ . Miletto *et al.* (2021) also
457 showed that microbial Mn(II) oxidation induces a Cr isotope fractionation of up to $+0.8 \pm 0.1\text{‰}$.

458 Therefore, the present results have to be considered as a first step toward a better comprehension of
459 Sb isotopes behaviour during redox processes in water.

460

461 5. Conclusion

462 In this study, isotopic fractionation generated by biotic and chemical Sb(III) oxidation into Sb(V) was
463 investigated for the first time. Important variations in Sb isotope fractionation occurred according to
464 the experimental conditions, showing either positive or negative fractionation, but always of low
465 amplitude. Biotic oxidation with a pure bacterial strain of the genus *Ensifer* was found to favour the
466 light isotopes of antimony in the oxidized phase, with a $\Delta^{123}\text{Sb}_{\text{Sb(V)}-\text{Sb(III)}}$ of $-0.20 \pm 0.07 \text{‰}$. This isotopic
467 fractionation could be related to kinetic fractionation that weakens over time rather than equilibrium
468 fractionation. This could reveal the occurrence of different steps in the oxidation of Sb(III) to Sb(V) via
469 biotic processes, and a competition between the equilibrium and kinetic fractionation. Regarding the
470 chemical oxidation of Sb(III) with H_2O_2 , Sb isotope fractionation reached $+0.3 \text{‰}$ in HCl medium; slight
471 enrichment in the heavy isotope in Sb(V) was attributed to a kinetic effect and multi-step reactions.
472 Investigations should be pursued further to document Sb isotope behaviour in a wide range of
473 environmental conditions.

474 6. Acknowledgements

475 This work received financial support from the CNRS INSU EC2CO program (Project AntiBol) and
476 ANR-22-CE01-0016 project ANTIMONY. We thank Léa Causse for trace element analysis performed on
477 the AETE-ISO platform, OSU OREME/University of Montpellier and David Clousier and Naoual Azhir el
478 Yousfi for their help during the experiments.

479 The authors warmly thank anonymous reviewers for their very relevant remarks and suggestions.

- 481 Asael, D. *et al.* (2007) 'Copper isotope fractionation in sedimentary copper mineralization (Timna
482 Valley, Israel)', *Chemical Geology*, 243(3), pp. 238–254. :
483 <https://doi.org/10.1016/j.chemgeo.2007.06.007>.
- 484 Battaglia-Brunet, F. *et al.* (2002) 'An arsenic(III)-oxidizing bacterial population: selection,
485 characterization, and performance in reactors', *Journal of Applied Microbiology*, 93(4), pp. 656–667. :
486 <https://doi.org/10.1046/j.1365-2672.2002.01726.x>.
- 487 Belzile, N., Chen, Y.-W. and Wang, Z. (2001) 'Oxidation of antimony (III) by amorphous iron and
488 manganese oxyhydroxides', *Chemical Geology*, 174(4), pp. 379–387. : [https://doi.org/10.1016/S0009-
489 2541\(00\)00287-4](https://doi.org/10.1016/S0009-2541(00)00287-4).
- 490 Bonner, N.A. and Oishi, W. (1961). Antimony in HCl Solutions. Kinetics of Complex Exchange and
491 Hydrolysis Reactions. In: Kinetics of complex exchange and hydrolysis reactions of antimony. Vol. 83,
492 pp. 85–99.
- 493 Criss, R.E. (1999) *Principles of Stable Isotope Distribution*. Oxford University Press, New York. Ducher,
494 M., Blanchard, M. and Balan, E. (2016) 'Equilibrium zinc isotope fractionation in Zn-bearing minerals
495 from first-principles calculations', *Chemical Geology*, 443, pp. 87–96. :
496 <https://doi.org/10.1016/j.chemgeo.2016.09.016>.
- 497 Dwivedi, P. *et al.* (2022) 'Oxidation of Dissolved Tetravalent Selenium by Birnessite: Se Isotope
498 Fractionation and the Effects of pH and Birnessite Structure', *Frontiers in Earth Science*, 10. :
499 <https://www.frontiersin.org/articles/10.3389/feart.2022.909900> (Accessed: 6 October 2022).
- 500 Ellis, A. *et al.* (2008) 'Environmental Cycling of Cr Using Stable Isotopes: Kinetic and Equilibrium Effects',
501 In AGU Fall Meeting Abstracts (Vol. 2008, pp. H53F–08).
- 502 Ferrari, C. *et al.* (2021) 'A single-step purification method for the precise determination of antimony
503 isotopic composition of environmental, geological and biological samples by HG-MC-ICP-MS', *Journal
504 of Analytical Atomic Spectrometry*, 36(Issue 4), pp. 776–785. : <https://doi.org/10.1039/D0JA00452A>.
- 505 Ferrari, C. *et al.* (2022) 'Equilibrium mass-dependent isotope fractionation of antimony between
506 stibnite and Sb secondary minerals: A first-principles study', *Chemical Geology*, p. 121115. :
507 <https://doi.org/10.1016/j.chemgeo.2022.121115>.
- 508 Filella, M., Belzile, N. and Chen, Y.-W. (2001) 'Antimony in the environment: a review focused on
509 natural waters. I. Occurrence', *Earth-Sciences Reviews*, 57, pp. 125–176.
- 510 Filella, M., Belzile, N. and Chen, Y.-W. (2002) 'Antimony in the environment: a review focused on
511 natural waters. II. Relevant solution chemistry', *Earth-Sciences Reviews*, 59, pp. 265–285.
- 512 Filella, M., Belzile, N. and Lett, M.-C. (2007) 'Antimony in the environment: a review focused on natural
513 waters. III. Microbial relevant interactions', *Earth Sciences Reviews*, 80, pp. 195–217. :
514 <https://doi.org/10.1016/j.earscirev.2006.09.003>.
- 515 Filella, M. and May, P.M. (2005) 'Critical appraisal of available thermodynamic data for the
516 complexation of antimony(III) and antimony(V) by low molecular mass organic ligands', *Journal of
517 Environmental Monitoring*, 7(12), pp. 1226–1237. : <https://doi.org/10.1039/B511453E>.

518 Fry, B. *et al.* (1988) 'Sulfur isotope effects associated with oxidation of sulfide by O₂ in aqueous
519 solution', *Chemical Geology: Isotope Geoscience section*, 73(3), pp. 205–210. :
520 [https://doi.org/10.1016/0168-9622\(88\)90001-2](https://doi.org/10.1016/0168-9622(88)90001-2).

521 Gilleaudeau, G.J. *et al.* (2016) 'Oxygenation of the mid-Proterozoic atmosphere: clues from chromium
522 isotopes in carbonates', *Geochemical Perspectives Letters*, 2(2), pp. 178–187. :
523 <https://doi.org/10.7185/geochemlet.1618>.

524 Goix, S. *et al.* (2011) 'Influence of source distribution and geochemical composition of aerosols on
525 children exposure in the large polymetallic mining region of the Bolivian Altiplano', *Science of The Total
526 Environment*, 412–413, pp. 170–184. : <https://doi.org/10.1016/j.scitotenv.2011.09.065>.

527 Guo, W. *et al.* (2018) 'Environmental geochemical and spatial/temporal behavior of total and
528 speciation of antimony in typical contaminated aquatic environment from Xikuangshan, China',
529 *Microchemical Journal*, 137, pp. 181–189. : <https://doi.org/10.1016/j.microc.2017.10.010>.

530 He, M. *et al.* (2019) 'Antimony speciation in the environment: Recent advances in understanding the
531 biogeochemical processes and ecological effects', *Journal of Environmental Sciences*, 75, pp. 14–39. :
532 <https://doi.org/10.1016/j.jes.2018.05.023>.

533 Herbel, M.J.; Johnson, T.M.; Oremland, R.S.; Bullen, T.D. (2000). 'Fractionation of selenium isotopes
534 during bacterial respiratory reduction of selenium oxyanions.' *Geochimica et Cosmochimica Acta*,
535 64(21), pp. 3701–3709. [https://doi.org/10.1016/S0016-7037\(00\)00456-7](https://doi.org/10.1016/S0016-7037(00)00456-7).

536 Hong, S. *et al.* (2012) 'Evidence of Global-Scale As, Mo, Sb, and Tl Atmospheric Pollution in the Antarctic
537 Snow', *Environmental Science & Technology*, 46(21), pp. 11550–11557. :
538 <https://doi.org/10.1021/es303086c>.

539 Johnson, T.M. (2004) 'A review of mass-dependent fractionation of selenium isotopes and implications
540 for other heavy stable isotopes', *Chemical Geology*, 204(3), pp. 201–214. :
541 <https://doi.org/10.1016/j.chemgeo.2003.11.015>.

542 Johnson, T.M. *et al.* (2022) 'A Review of the Development of Cr, Se, U, Sb, and Te Isotopes as Indicators
543 of Redox Reactions, Contaminant Fate, and Contaminant Transport in Aqueous Systems', in *Isotopic
544 Constraints on Earth System Processes*. American Geophysical Union (AGU), pp. 237–269. :
545 <https://doi.org/10.1002/9781119595007.ch10>.

546 Johnston, S.G. *et al.* (2020) 'Antimony and arsenic speciation, redox-cycling and contrasting mobility in
547 a mining-impacted river system', *Science of The Total Environment*, 710, p. 136354. :
548 <https://doi.org/10.1016/j.scitotenv.2019.136354>.

549 Kimball, B.E. *et al.* (2009) 'Copper isotope fractionation in acid mine drainage', *Geochimica et
550 Cosmochimica Acta*, 73(5), pp. 1247–1263. : <https://doi.org/10.1016/j.gca.2008.11.035>.

551 Krachler, M. *et al.* (2005) 'Increasing atmospheric antimony contamination in the northern
552 hemisphere: snow and ice evidence from Devon Island, Arctic Canada', *Journal of Environmental
553 Monitoring*, 7(12), pp. 1169–1176. : <https://doi.org/10.1039/B509373B>.

554 Larson, P.B. *et al.* (2003) 'Copper isotope ratios in magmatic and hydrothermal ore-forming
555 environments', *Chemical Geology*, 201(3), pp. 337–350. :
556 <https://doi.org/10.1016/j.chemgeo.2003.08.006>.

- 557 Lehr, C.R., Kashyap, D.R. and McDermott, T.R. (2007) 'New Insights into Microbial Oxidation of
558 Antimony and Arsenic', *Applied and Environmental Microbiology*, 73(7), pp. 2386–2389. :
559 <https://doi.org/10.1128/AEM.02789-06>.
- 560 Leuz, A.-K. and Johnson, C.A. (2005) 'Oxidation of Sb(III) to Sb(V) by O₂ and H₂O₂ in aqueous solutions',
561 *Geochimica et Cosmochimica Acta*, 69(5), pp. 1165–1172. : <https://doi.org/10.1016/j.gca.2004.08.019>.
- 562 Leuz, A.-K., Mönch, H. and Johnson, A. (2006) 'Sorption of Sb(III) and Sb(V) to Goethite: Influence on
563 Sb(III) Oxidation and Mobilization', *Environement Sciences and Technologies*, 40(23), pp. 7277–7282. :
564 <https://doi.org/10.1021/es061284b>.
- 565 Leverett, P. *et al.* (2012) 'Tripuhyite and schafarzikite: two of the ultimate sinks for antimony in the
566 natural environment', *Mineralogical Magazine*, 76(4), pp. 891–902. :
567 <https://doi.org/10.1180/minmag.2012.076.4.06>.
- 568 Li, J. *et al.* (2013) 'Phylogenetic and genome analyses of antimony-oxidizing bacteria isolated from
569 antimony mined soil', *International Biodeterioration & Biodegradation*, 76, pp. 76–80. :
570 <https://doi.org/10.1016/j.ibiod.2012.06.009>.
- 571 Li, J. *et al.* (2015) 'Proteomics and Genetics for Identification of a Bacterial Antimonite Oxidase in
572 *Agrobacterium tumefaciens*', *Environmental Science & Technology*, 49(10), pp. 5980–5989. :
573 <https://doi.org/10.1021/es506318b>.
- 574 Li, J. *et al.* (2018) 'Novel Hyper Antimony-Oxidizing Bacteria Isolated from Contaminated Mine Soils in
575 China', *Geomicrobiology Journal*, 35(8), pp. 713–720. :
576 <https://doi.org/10.1080/01490451.2018.1454556>.
- 577 Li, X. and Liu, Y. (2011) 'Equilibrium Se isotope fractionation parameters: A first-principles study', *Earth
578 and Planetary Science Letters*, 304(1), pp. 113–120. : <https://doi.org/10.1016/j.epsl.2011.01.022>.
- 579 Liu, S. *et al.* (2021) 'Equilibrium Cu isotope fractionation in copper minerals: a first-principles study',
580 *Chemical Geology*, 564, p. 120060. : <https://doi.org/10.1016/j.chemgeo.2021.120060>.
- 581 Mackinney, J.S. (2016) *Antimony isotopes as indicator of RedOx reactions in aqueous systems:
582 fractionation during Sb(V) reduction by sulfide and isotope exchange kinetics between dissolved Sb(III)
583 and Sb(V)*. Thesis. University of Illinois at Urbana-Champaign. :
584 <https://core.ac.uk/download/pdf/158314035.pdf>.
- 585 Maréchal, C.N., Télouk, P. and Albarède, F. (1999) 'Precise analysis of copper and zinc isotopic
586 compositions by plasma-source mass spectrometry', *Chemical Geology*, 156(1), pp. 251–273. :
587 [https://doi.org/10.1016/S0009-2541\(98\)00191-0](https://doi.org/10.1016/S0009-2541(98)00191-0).
- 588 Mathur, R. *et al.* (2005) 'Cu isotopic fractionation in the supergene environment with and without
589 bacteria', *Geochimica et Cosmochimica Acta*, 69(22), pp. 5233–5246. :
590 <https://doi.org/10.1016/j.gca.2005.06.022>.
- 591 Mathur, R. *et al.* (2009) 'Exploration potential of Cu isotope fractionation in porphyry copper deposits',
592 *Journal of Geochemical Exploration*, 102(1), pp. 1–6. : <https://doi.org/10.1016/j.gexplo.2008.09.004>.
- 593 Mathur, R. *et al.* (2010) 'Patterns in the Copper Isotope Composition of Minerals in Porphyry Copper
594 Deposits in Southwestern United States', *Economic Geology*, 105(8), pp. 1457–1467. :
595 <https://doi.org/10.2113/econgeo.105.8.1457>.

596 Miletto, M. *et al.* (2021) 'Marine microbial Mn(II) oxidation mediates Cr(III) oxidation and isotope
597 fractionation', *Geochimica et Cosmochimica Acta*, 297, pp. 101–119. :
598 <https://doi.org/10.1016/j.gca.2021.01.008>.

599 Mitsunobu, S., Harada, T. and Takahashi, Y. (2006) 'Comparison of Antimony Behavior with that of
600 Arsenic under Various Soil Redox Conditions', *Environmental Science & Technology*, 40(23), pp. 7270–
601 7276. : <https://doi.org/10.1021/es060694x>.

602 Moynier, F. *et al.* (2017) 'The Isotope Geochemistry of Zinc and Copper', *Reviews in Mineralogy and
603 Geochemistry*, 82(1), pp. 543–600. : <https://doi.org/10.2138/rmg.2017.82.13>.

604 Mukhopadhyay, R. *et al.* (2002) 'Microbial arsenic: from geocycles to genes and enzymes', *FEMS
605 Microbiology Reviews*, 26(3), pp. 311–325. : <https://doi.org/10.1111/j.1574-6976.2002.tb00617.x>.

606 Nguyen, V.K. *et al.* (2017) 'Microbial oxidation of antimonite and arsenite by bacteria isolated from
607 antimony-contaminated soils', *International Journal of Hydrogen Energy*, 42(45), pp. 27832–27842. :
608 <https://doi.org/10.1016/j.ijhydene.2017.08.056>.

609 Nguyen, V.K. and Lee, J.-U. (2015) 'Antimony-Oxidizing Bacteria Isolated from Antimony-Contaminated
610 Sediment – A Phylogenetic Study', *Geomicrobiology Journal*, 32(1), pp. 50–58. :
611 <https://doi.org/10.1080/01490451.2014.925009>.

612 Quentel, F. *et al.* (2004) 'Kinetic Studies on Sb(III) Oxidation by hydrogen Peroxide in Aqueous Solution',
613 *Environmental Science and Technology*, 38(10), pp. 2843–2848. : <https://doi.org/10.1021/es035019r>.

614 Ratie, G. *et al.* (2021) 'Cadmium isotope fractionation during complexation with humic acid',
615 *Environmental Science & technology*, 55 (11), pp.7430-7444. :
616 <https://doi.org/10.1021/acs.est.1c00646>.

617 Resongles, E. *et al.* (2013) 'Fate of Sb(V) and Sb(III) species along a gradient of pH and oxygen
618 concentration in the Canoulès mine waters (Southern France)', *Environmental Science Processes and
619 Impacts*, 15, pp. 1536–1544. : <https://doi.org/10.1039/c3em00215b>.

620 Rodushkin, I. *et al.* (2004) 'Isotopic Fractionation during Diffusion of Transition Metal Ions in Solution',
621 *Analytical Chemistry*, 76(7), pp. 2148–2151. : <https://doi.org/10.1021/ac035296g>.

622 Roper, A.J., Williams, P.A. and Filella, M. (2012) 'Secondary antimony minerals: Phases that control the
623 dispersion of antimony in the supergene zone', *Geochemistry*, 72, pp. 9–14. :
624 <https://doi.org/10.1016/j.chemer.2012.01.005>.

625 Rouxel, O., Ludden, J. and Fouquet, Y. (2003) 'Antimony isotope variations in natural systems and
626 implications for their use as geochemical tracers', *Chemical Geology*, 200, pp. 25–40. :
627 [https://doi.org/10.1016/S0009-2541\(03\)00121-9](https://doi.org/10.1016/S0009-2541(03)00121-9)

628 Santini, J.M. and vanden Hoven, R.N. (2004) 'Molybdenum-Containing Arsenite Oxidase of the
629 Chemolithoautotrophic Arsenite Oxidizer NT-26', *Journal of Bacteriology*, 186(6), pp. 1614–1619. :
630 <https://doi.org/10.1128/jb.186.6.1614-1619.2004>.

631 Schauble, E.A. (2004) 'Applying Stable Isotope Fractionation Theory to New Systems', *Reviews in
632 Mineralogy and Geochemistry*, 55(1), pp. 65–111. : <https://doi.org/10.2138/gsrmg.55.1.65>.

633 Schilling, K. *et al.* (2020) 'Mass-dependent selenium isotopic fractionation during microbial reduction
634 of seleno-oxyanions by phylogenetically diverse bacteria', *Geochimica et Cosmochimica Acta*, 276, pp.
635 274–288. : <https://doi.org/10.1016/j.gca.2020.02.036>.

636 Sen, I.S. and Peucker-Ehrenbrink, B. (2012) 'Anthropogenic Disturbance of Element Cycles at the
637 Earth's Surface', *Environmental Science & Technology*, 46(16), pp. 8601–8609. :
638 <https://doi.org/10.1021/es301261x>.

639 Stephens, J.A. *et al.* (2021) 'Use of non-traditional heavy stable isotopes in archaeological research',
640 *Journal of Archaeological Science*, 127, p. 105334. : <https://doi.org/10.1016/j.jas.2021.105334>.

641 Tanimizu, M. *et al.* (2011) 'Determination of natural isotopic variation in antimony using inductively
642 coupled plasma mass spectrometry for an uncertainty estimation of the standard atomic weight of
643 antimony', *Geochemical Journal*, 45, pp. 27–32.

644 Tella, M. and Pokrovski, G.S. (2009) 'Antimony(III) complexing with O-bearing organic ligands in
645 aqueous solution: An X-ray absorption fine structure spectroscopy and solubility study', *Geochimica et
646 Cosmochimica Acta*, 73(2), pp. 268–290. : <https://doi.org/10.1016/j.gca.2008.10.014>.

647 Terry, L.R. *et al.* (2015) 'Microbial Oxidation of Antimony(III) with Oxygen or Nitrate by Bacteria Isolated
648 from Contaminated Mine Sediments', *Applied and Environmental Microbiology*, 81(24), pp. 8478–
649 8488. : <https://doi.org/10.1128/AEM.01970-15>.

650 Thullner, M. *et al.* (2013) 'Influence of mass transfer on stable isotope fractionation', *Applied
651 Microbiology and Biotechnology*, 97(2), pp. 441–452. : <https://doi.org/10.1007/s00253-012-4537-7>.

652 Torma, A.E. and Habashi, F. (1972) 'Oxidation of copper (II) selenide by *Thiobacillus ferrooxidans*',
653 *Canadian Journal of Microbiology* [Preprint]. : <https://doi.org/10.1139/m72-278>.

654 Vink, B.W. (1996) 'Stability relations of antimony and arsenic compounds in the light of revised and
655 extended Eh-pH diagrams', *Chemical Geology*, 130(1), pp. 21–30. : [https://doi.org/10.1016/0009-
656 2541\(95\)00183-2](https://doi.org/10.1016/0009-6541(95)00183-2).

657 Wang, D.T. *et al.* (2010) 'Stable Isotope Fractionation during Chromium(III) Oxidation by δ -MnO₂', In:
658 American Geophysical Union, Fall Meeting 2010, abstract id. H53F-1109.

659 Wang, Q. *et al.* (2015) 'Arsenite Oxidase Also Functions as an Antimonite Oxidase', *Applied and
660 Environmental Microbiology*, 81(6). : <https://doi.org/10.1128/AEM.02981-14>.

661 Wang, L., Ye, L., Yin, Z., Zhang, L., Jing, C. (2022). 'Antimonite oxidation by microbial extracellular
662 superoxide in *Pseudomonas* sp. SbB1'. *Geochimica et Cosmochimica Acta*, 316, pp. 122-134.

663 Wiederhold, J.G. (2015) 'Metal Stable Isotope Signatures as Tracers in Environmental Geochemistry',
664 *Environmental Science & Technology*, 49(5), pp. 2606–2624. : <https://doi.org/10.1021/es504683e>.

665 Wiggerhauser, M.; Moore, R.E.T.; Wang, P.; Bienert, G.P.; Laursen, K. H.; Blotvogel, S. (2022). 'Stable
666 Isotope Fractionation of Metals and Metalloids in Plants: A Review.' *Frontiers in Plant Science*.
667 13:840941. <https://doi.org/10.3389/fpls.2022.840941>.

668

669 Xi, J. *et al.* (2015) 'Comparison of masking agents for antimony speciation analysis using hydride
670 generation atomic fluorescence spectrometry', *Frontiers of Environmental Science & Engineering*, 9(6),
671 pp. 970–978. : <https://doi.org/10.1007/s11783-014-0716-3>.

- 672 Yu, M.-Q., Liu, G.-Q. and Jin, Q. (1983) 'Determination of trace arsenic, antimony, selenium and
673 tellurium in various oxidation states in water by hydride generation and atomic-absorption
674 spectrophotometry after enrichment and separation with thiol cotton', *Talanta*, 30(4), pp. 265–270.
675 [https://doi.org/10.1016/0039-9140\(83\)80060-5](https://doi.org/10.1016/0039-9140(83)80060-5).
- 676 Zhang, J. *et al.* (2022) 'Oxidation of organoarsenicals and antimonite by a novel flavin monooxygenase
677 widely present in soil bacteria', *Environmental Microbiology*, 24(2), pp. 752–761. :
678 <https://doi.org/10.1111/1462-2920.15488>.
- 679 Zhang, Y. *et al.* (2018) 'Cadmium isotopic evidence for the evolution of marine primary productivity
680 and the biological extinction event during the Permian-Triassic crisis from the Meishan section, South
681 China', *Chemical Geology*, 481, pp. 110–118. : <https://doi.org/10.1016/j.chemgeo.2018.02.005>.
- 682 Zhou, W. *et al.* (2023) 'Antimony Isotope Fractionation Revealed from EXAFS during Adsorption on Fe
683 (Oxyhydr)oxides', *Environmental Science & Technology*, 57(25), pp. 9353–9361. :
684 <https://doi.org/10.1021/acs.est.3c01906>.
- 685 Zhu, J. *et al.* (2009) 'Environmental characteristics of water near the Xikuangshan antimony mine.',
686 *Acta Scientiae Circumstantiae*, 29.
- 687 Zink, S., Schoenberg, R. and Staubwasser, M. (2010) 'Isotopic fractionation and reaction kinetics
688 between Cr(III) and Cr(VI) in aqueous media', *Geochimica et Cosmochimica Acta*, 74(20), pp. 5729–
689 5745. : <https://doi.org/10.1016/j.gca.2010.07.015>.
- 690
- 691

692 **Antimony isotopic fractionation during Sb(III) to Sb(V) oxidation:**
693 **biotic and abiotic perspectives**

694 Supplementary Information

695 Colin Ferrari^a, Eléonore Resongles^a, Marina Héry^a, Angélique Désoeuvre^a, Rémi Freydier^a, Sophie
696 Delpoux^a, Odile Bruneel^a, Corinne Casiot^{a*}

697 ^a*HydroSciences Montpellier, Univ. Montpellier, CNRS, IRD, Montpellier, France*

698

699 *Corresponding author

700 Mailing address : HydroSciences Montpellier UMR 5151

701 Faculté des Sciences Pharmaceutiques et Biologiques

702 Université de Montpellier, Bât. Hydropolis

703 15, avenue Charles Flahault

704 34093 Montpellier cedex 05, France

705 Email : corinne.casiot-marouani@umontpellier.fr

706

707 This PDF file includes: Tables S1 to S3 and Figures S1 to S4.

Additional tables:

Table S1: Recovery rate of pure Sb(III) and pure Sb(V) solutions on TSP.

Solution	Step	[Sb] loaded/eluted (ng)	Yield (%)	Total Sb recovered (%)
Pure Sb(V) solution	Initial loaded solution	Sb(V) 448		
	Sb(V) collection	408	91.1	92.7
	Sb(III) collection	7.6		
Pure Sb(III) solution	Initial loaded solution =	Sb(III) 488		
	Sb(V) collection	< QL		
	Sb(III) collection	507	103.8	103.8

Table S2: Comparison between the percentage of oxidation calculated through HPLC and recovered through the physical separation of Sb(III) and Sb(V) on TSP.

Ech	Sb(III)/Sb(V)	HPLC measurement		TSP separation	Difference (%)
		[Sb] (%)	[Sb] (%)	[Sb] (%)	
RDB1 t=0	Sb(III)	98.3	98.1	98.1	0.3
	Sb(V)	1.7	1.9	1.9	
RDB1 t = 24	Sb(III)	86.6	88.6	88.6	-2.0
	Sb(V)	13.4	11.4	11.4	
RDB1 t=30h	Sb(III)	72.3	67.3	67.3	5.0
	Sb(V)	27.7	32.7	32.7	
RDB t=30h	Sb(III)	72.6	69.4	69.4	3.2
	Sb(V)	27.4	30.6	30.6	
RDB3 t=30h	Sb(III)	68.1	69.7	69.7	-1.6
	Sb(V)	31.9	30.3	30.3	
RDB4 t=39h	Sb(III)	54.5	57.2	57.2	-2.7
	Sb(V)	45.5	42.8	42.8	
RDB4 t=42h	Sb(III)	43.6	47.6	47.6	-4.0
	Sb(V)	56.4	52.4	52.4	
RDB4 t=47h	Sb(III)	25.2	33.7	33.7	-8.5
	Sb(V)	74.8	66.3	66.3	
RDB1 t=47h	Sb(III)	13.9	24.9	24.9	-11.1
	Sb(V)	86.1	75.1	75.1	
RDB3 t=47h	Sb(III)	5.7	19.1	19.1	-13.5
	Sb(V)	94.3	80.9	80.9	

Table S3: $\delta^{123}\text{Sb}$ of the Sb(III) and Sb(V) species physically separated on TSP in the same H_2O_2 , Sb and NaNO_3 concentrations than the online experiment described in 2.2.2 Chemical oxidation, but at pH 9.

	Time (min)	Oxidation (%)	$\delta^{123}\text{Sb}$ (‰)	2 sd (‰)
Sb(III)	25	10	0.34	0.01
	70	18	0.33	0.01
	140	19	0.33	0.04
Sb(V)	25	10	0.35	0.05
	70	18	0.34	0.06
	140	19	0.31	0.06

Additional figures:

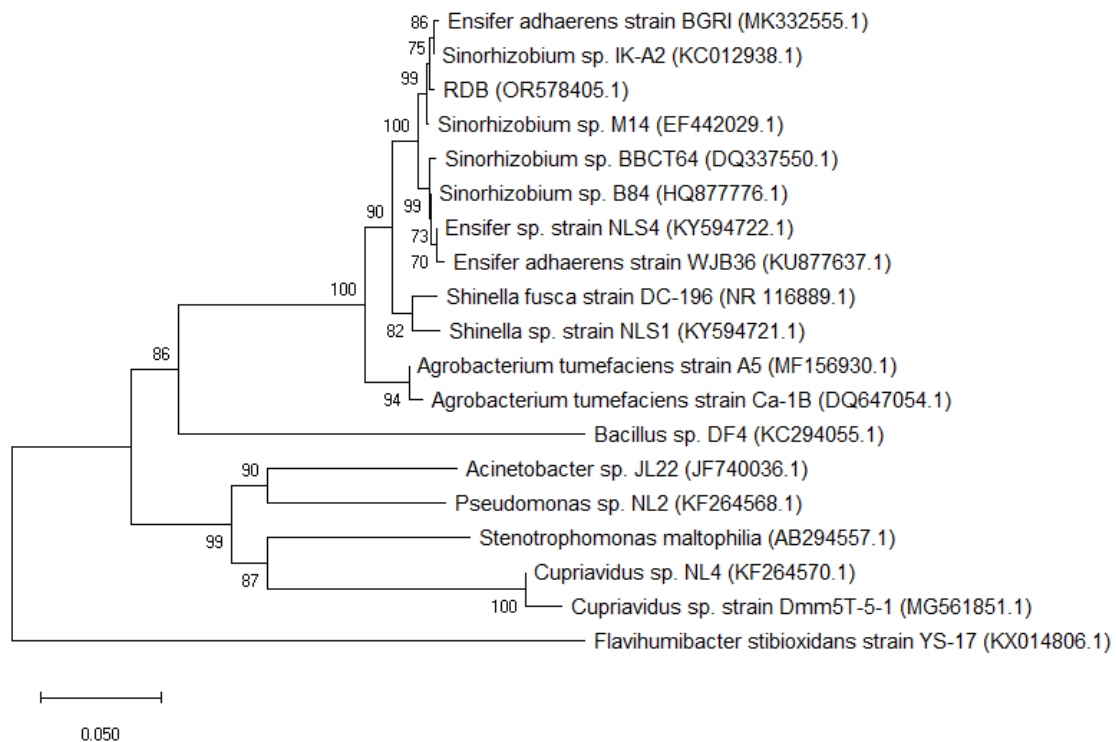


Figure S1: Phylogenetic tree constructed with the 16S rRNA sequences from RDB, its two closest relatives and other *Sb(III)* oxidizing bacteria. It was made with MEGAX (Kumar et al., 2018), using the neighbor-joining method and the Kimura correction. Nodal robustness of the tree was assessed using 1000 bootstrap replicates. DNA was extracted from RDB culture using the DNeasy PowerWater Kit (Qiagen, Hilden, Germany), according to the manufacturer's instructions. 16S rRNA gene was amplified using primers 8f (Lane 1991) and 1489r (Weisburg et al., 1991) primers. Sequencing of both DNA strands was performed by GATC Biotech (Konstanz, Germany). A 1371 bp consensus sequences was obtained from the alignment of the two sequenced brands and deposited in Genbank under the accession number OR578405. References: Lane DJ (1991) rRNA sequencing. In Stachenbradt GME (ed) *Nucleic acid techniques in bacterial systematics*. Wiley, Chichester, United Kingdom pp115-175. Weisburg, W.G., S.M. Barns, D.A.Pelletier, and D.J. Lane. 1991. 16S ribosomal DNA amplification for phylogenetic study. *J. Bacteriol.* 173 :697-703. Kumar S., Stecher G., Li M., Knyaz C., and Tamura K. (2018). MEGA X: Molecular Evolutionary Genetics Analysis across computing platforms. *Molecular Biology and Evolution* 35:1547-1549.

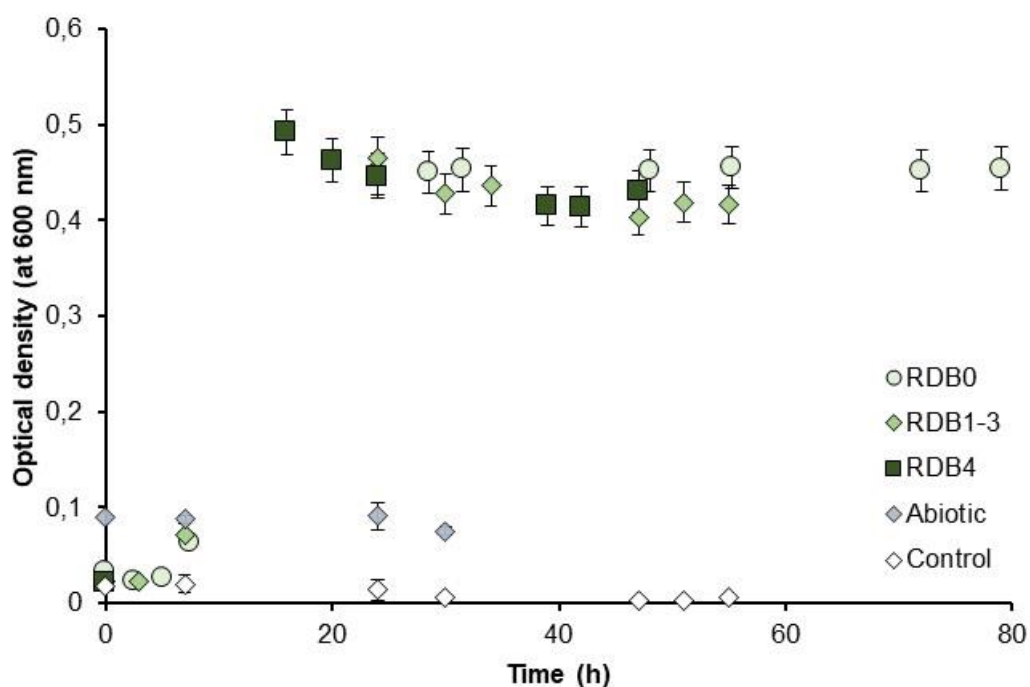


Figure S2: Optical Density measured at 600 nm for biotic (green diamonds), abiotic (light blue triangles), and control (dark blue triangles) batch.

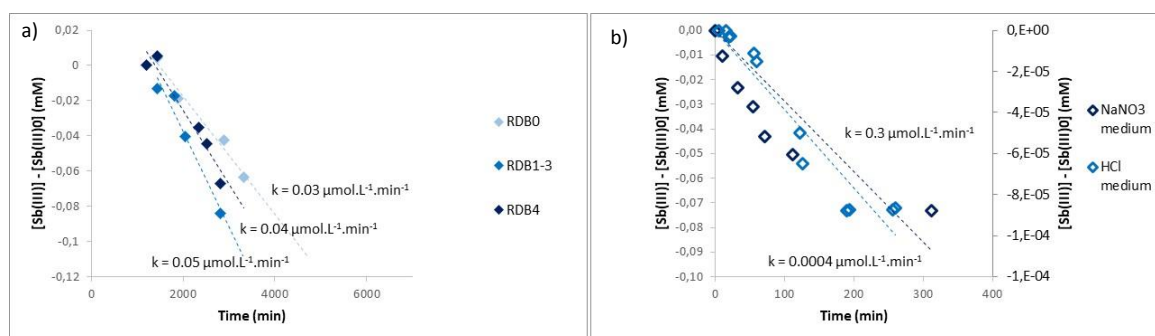


Figure S3 – Variation of Sb(III) concentration as a function of time in (a) biotic oxidation experiments exhibiting Sb(III) oxidation rate values of $0.05 \mu\text{mol.L}^{-1}.\text{min}^{-1}$ (RDB1-3), $0.04 \mu\text{mol.L}^{-1}.\text{min}^{-1}$ (RDB4) and $0.03 \mu\text{mol.L}^{-1}.\text{min}^{-1}$ (RDB0) - and (b) chemical oxidation experiments exhibiting Sb(III) oxidation rate values of $0.3 \mu\text{mol.L}^{-1}.\text{min}^{-1}$ (for NaNO_3 medium) and $0.0004 \mu\text{mol.L}^{-1}.\text{min}^{-1}$ (for HCl medium). The kinetic constant k (considering a zero-order rate law) is mentioned.

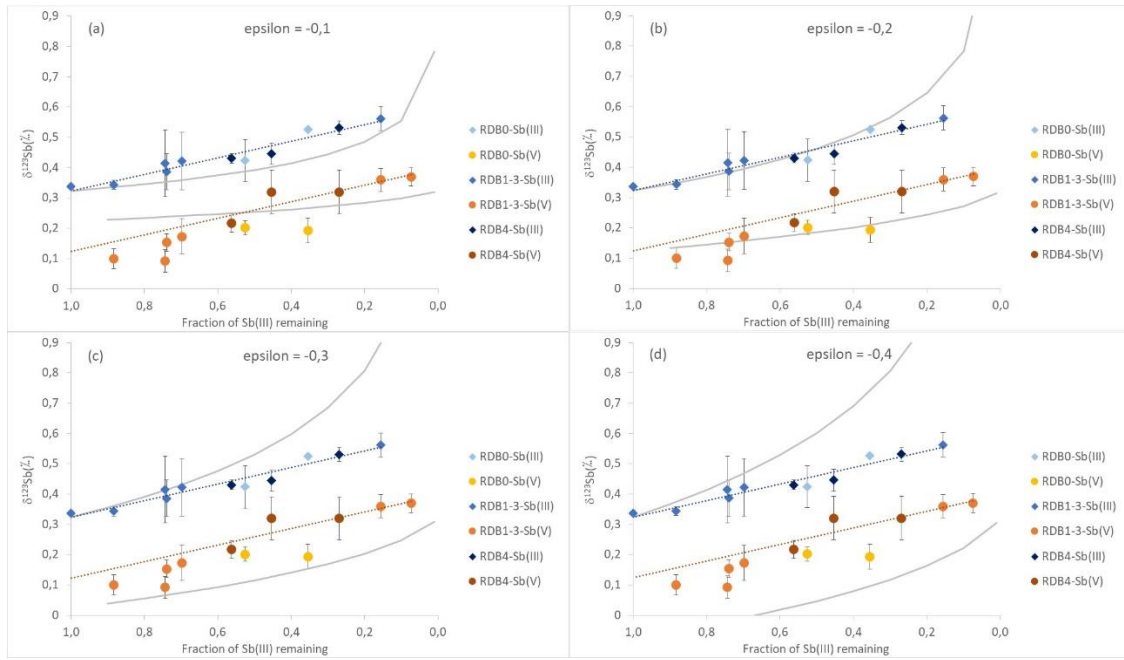


Figure S4 – Representation of Rayleigh model ($\delta^{123}\text{Sb}$ of reactant Sb(III) and cumulative product Sb(V) in grey lines) for different fractionation factors epsilon $\epsilon = -0.1$ (a), -0.2 (b), -0.3 (c) and -0.4 (d).

